

## NUMERICAL SIMULATION OF CHANGES IN MICROGRAVITY AND ELECTROKINETIC POTENTIALS ASSOCIATED WITH THE EXPLOITATION OF THE ONIKOBE GEOTHERMAL FIELD, MIYAGI PREFECTURE, JAPAN

Shigetaka Nakanishi

Electric Power Development Company  
Tokyo, 104-8165, Japan  
shigetaka\_nakanishi@epdc.co.jp

John W. Pritchett

Maxwell Technologies  
San Diego, California, 92123-1506, USA  
john@maxwell.com

Shigeyuki Yamazawa

New Energy and Industrial Technology Development Organization  
Tokyo, 170-6028, Japan  
yamazawasgy@nedo.go.jp

### **ABSTRACT**

This paper presents the results of a feasibility study to appraise the practicality of using geophysical techniques to detect and characterize subsurface changes induced in geothermal reservoir by field operations. A numerical model of the Onikobe geothermal reservoir (Japan) was developed. The modeling study involved (a) developing a stable solution for the natural state of the field prior to the beginning of field operations in 1975, (b) imposing the known fluid production and injection histories based on field records of well flow rates for the period March 1975 – January 1997, and then (c) assuming that well flow rates remain fixed thereafter, forecasting the future response of the reservoir for an additional ten years.

Then, the STAR microgravity and electrokinetic potential postprocessors were applied to the reservoir model to calculate the probable changes that will be observable at the surface using these geophysical survey techniques. The strength and spatial distribution of the signals were estimated and the practicality of detecting such signals in the field was appraised. The Onikobe field appears to be a marginal prospect for the utilization of microgravity measurements for future reservoir monitoring based on these calculations, since most of the major microgravity changes have already taken place in the now-mature field. It was estimated, on the other hand, that substantial changes in surface SP started taking place in about 1983, and that these changes are continuing to the present day as a result of the ongoing temporal evolution of the brine production-injection scheme.

### **INTRODUCTION**

The New Energy and Industrial Technology Development Organization (“NEDO”; an agency of the Japanese Government) has carried out numerous projects over the years to promote the development of geothermal resources. Most recently, starting in 1997, NEDO has undertaken a new initiative: “Development of Technology for Reservoir Mass and Heat Flow Characterization” (Horikoshi *et al.*, 1998). As a part of this new project, development of “Integrated reservoir modeling and simulation techniques” (Nakanishi *et al.*, 2000) has been undertaken. This involves developing new analysis techniques for the various geophysical data sets and combining them with traditional reservoir engineering practice.

As a part of this effort, we have carried out various “feasibility studies” to appraise the practicality of using these geophysical techniques (particularly the monitoring of changes in microgravity and ground-surface self-potential) to detect and characterize subsurface changes induced in geothermal reservoirs by field operations. These feasibility studies involve (1) adopting a particular mathematical “reservoir model” for the system, (2) using that model to perform calculations of changes in underground conditions over a period of many years of operation, and then (3) using mathematical “postprocessors” (Pritchett (1995), and Ishido and Pritchett (1999)) to calculate the probable changes which will be observable at the surface using the geophysical survey techniques. Pritchett *et al.* (2000) describe the results of one of these studies for a “hypothetical” (but typical) high-enthalpy geothermal reservoir.

This paper presents the results of a similar feasibility study for the Onikobe reservoir system; a mature field which has been supplying power to the grid since 1975. In the study, the strength and spatial distribution of the geophysical signals were estimated and the practicality of detecting such signals in the field was appraised.

### **THE ONIKOBE GEOTHERMAL FIELD**

The Onikobe geothermal field, located in Miyagi prefecture in Japan, has been developed and produced at a capacity of 12.5 MWe by the Electric Power Development Company (EPDC) since 1975. The Onikobe geothermal wellfield is shown in Fig.1. Abe (1988) and Klein et al. (1990) provide a detailed description of the geological setting and the conceptual model of the field, summarized below. The field is located within the 2 million years old Onikobe caldera (about 8 km in diameter). The younger Katayama structural dome (3km × 0.5km) occupies the southeastern part of the caldera.



Figure 1. Production and injection well locations in the Onikobe geothermal field.

A triangular 200-meter topographic depression (1.5 km × 0.5 km) has formed on top of the Katayama dome, drained by the southward-flowing Ofuka River. This depression is believed to be a downfaulted block resulting from extensional stresses associated with the formation of the dome. The faults are believed to provide the vertical fluid conduits which charge the Onikobe geothermal reservoir. Areas of extensive surface activity and acid alteration are found along the northern and western sides of the triangular depression (the “Katayama thermal area”). The Onikobe wellfield is situated in the Katayama thermal area. The Katayama thermal area is encircled by other natural thermal discharge areas at radii of two to three kilometers. The present investigation focuses on the “study area” shown in Fig.2, which illustrates these features. The wellfield itself is quite small; the “project area” containing the wellheads and the power station occupies only 0.14 km<sup>2</sup>,

although the entire area penetrated by the deviated production and injection wells represents around 1 km<sup>2</sup>.

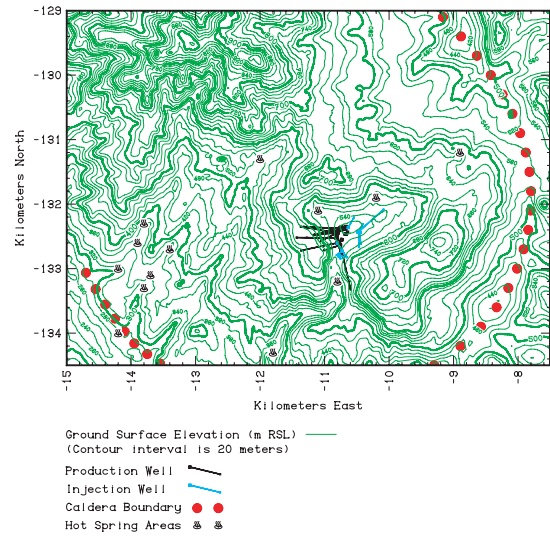


Figure 2. Map of the Onikobe study area.

The 24-year performance history of the Onikobe reservoir involves two principal phenomenological characteristics. The first is the evolution of drilling practice to maintain field operations. All of the early production wells were drilled vertically and completed in the “shallow” two phase reservoir, because strongly acidic fluids which were unsuitable for use in the plant were encountered at deeper levels during exploration (Abe, 1988). This early steam production was not sustainable, however, and steam production from the shallow reservoir declined with a continuous decline in enthalpy. Then, in 1980, it was discovered that deeper wells, if deviation-drilled away from the center of the anomaly (see Fig. 1), could also produce substantial quantities of hot liquid brines of near-neutral pH. Accordingly, starting in about 1982, production was shifted to these deeper deviated wells. By 1988, the new deep deviation-drilling program had succeeded in returning the field’s generating capacity to 12.5 MWe, and this level of performance is still being sustained, although several make-up wells have been drilled since that time. The second noteworthy characteristic of the reservoir production history involves significant temporal changes in geochemical compositions of the produced fluids. Temporal shifts in geochemistry have been observed corresponding to changes in the production/injection scheme and reflecting the significant spatial variations of the chemical compositions of the geothermal fluids in the reservoir. These changes appear to reflect the effects of both natural and artificial convection and rock/water interactions, downflows of meteoric surface waters into the underlying reservoir system, and mixing of concentrated reinjected brines into the ambient reservoir waters.

## THE MATHEMATICAL RESERVOIR MODEL

### Model Description

Recently, a mathematical model of the Onikobe field and the surrounding area was developed by Nakanishi and Iwai (2000) using the STAR geothermal reservoir simulator (Pritchett, 1995). The modeling study involved (a) developing a stable solution for the natural state of the field prior to the beginning of field operations in March 1975, (b) imposing the known fluid production and injection histories based on field records of well flow rates for the period 1 March 1975 – 1 January 1997, and then (c) assuming that well flow rates remain fixed thereafter, forecasting the future response of the reservoir for an additional ten years (from 1 January 1997 to 1 January 2007).

The model covers 52 km<sup>2</sup> (slightly greater than that of the “study area”) in the southern part of the Onikobe caldera, extending 8 km in the east-west direction and 6.5 km in the north-south direction (Fig. 3). The spatial discretization is rather coarse with 11 grid blocks in the east-west direction (“i” index) and 10 blocks in the north-south direction (“j” index). Grid block dimensions vary between 0.3 and 2.0 km in the E – W direction and between 0.2 and 1.5 km in the N – S direction, with the highest resolution applied near the Onikobe borefield. Vertically the model extends from the earth surface (ranging from +200 m to + 400m above sea level – “ASL”) to –2,000 m ASL. A total of 14 layers (“k” index) were used, with ten layers (each 200 m thick) between sea level and –2,000 m ASL, and four layers (each 100 m thick) above sea level. Some of the uppermost grid blocks are “void”; the total number of non-void blocks is 1,406. The total volume of these non-void blocks is 117 km<sup>3</sup>.

The northern vertical boundary and the eastern vertical boundary were both treated as impermeable and insulated. By contrast, constant hydrostatic pressure boundary conditions were imposed on the southern and western vertical grid boundaries. Pressures were also prescribed along the upper surfaces of the topmost grid blocks to permit vertical discharge and recharge of fluid and exchange of reservoir brine with the shallow groundwater system. The bottom boundary of the computational volume was mainly treated as impermeable with a constant uniform upward heat flux (175 mW/m<sup>2</sup>). Mass sources to represent the upwelling flow underlying the Katayama area were distributed in a restricted part of the bottom boundary. The spatial distribution, temperature and strength of these mass sources as well as permeability distribution throughout the system were used as the main fitting parameters in

the natural-state simulation. A fixed uniform upward flux of hot (330°C) liquid water totaling 10 kg/s was finally imposed within a 2.25 km<sup>2</sup> area (-11.5 km E < x < -10 km E, -133.5 km N < y < -132 km N) as indicated in Fig.3.

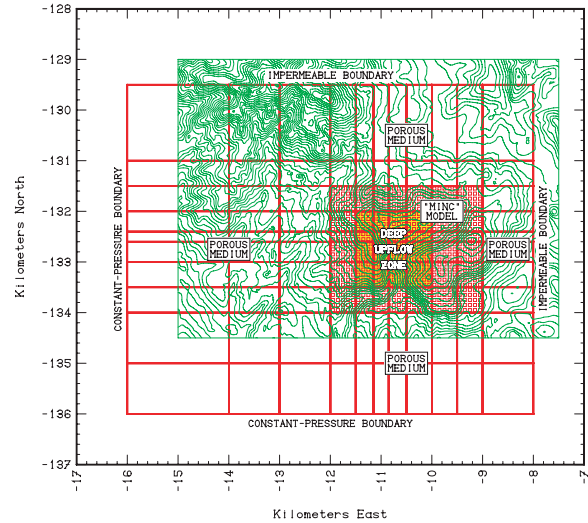


Figure 3. Plan view of the “study area” and the computational grid. Textured area uses “MINC” double-porosity representation. Yellow area shows region of deep hot water inflow.

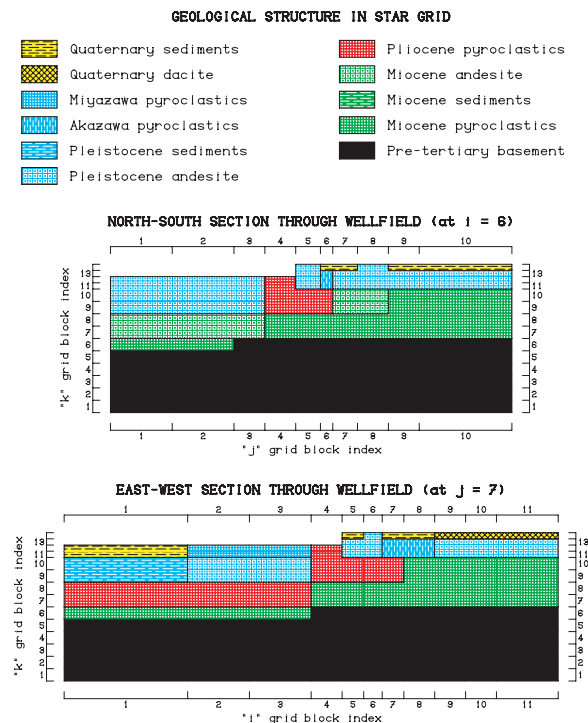


Figure 4. Geological structure of the reservoir model in vertical planes passing through the wellfield.

Rock properties other than permeability (porosity, specific heat, thermal conductivity and density) used as input to the model were based on measured data for each rock type. Fig. 4 shows how the various major formations were assigned in the north-south section at “i=6” and the east-west section at “j=7”. The values of the “bulk properties” of these formations were shown in Table 1. The distribution of the absolute permeability was established as a part of the “free parameter” variation process during the simulation. The permeability values that were finally adopted are summarized in Table 2.

Table 1. Bulk properties of geological formations in the simulation model.

| FORMATION             | FORMATION POROSITY | PROPERTIES OF ROCK GRAIN MATERIALS |                               |                        |
|-----------------------|--------------------|------------------------------------|-------------------------------|------------------------|
|                       |                    | Mass Density (g/cm <sup>3</sup> )  | Thermal Conductivity (W/m·°C) | Heat Capacity (J/g·°C) |
| Quaternary sediments  | 8%                 | 2.2                                | 1.82                          | 1                      |
| Quaternary dacite     | 9%                 | 2.2                                | 1.59                          | 1                      |
| Miyazawa pyroclastics | 18%                | 2.1                                | 0.75                          | 1                      |
| Akazawa pyroclastics  | 21%                | 2.2                                | 0.71                          | 1                      |
| Pleistocene sediments | 11%                | 2.1                                | 2.40                          | 1                      |
| Pleistocene andesite  | 10%                | 2.4                                | 1.34                          | 1                      |
| Pliocene pyroclastics | 30%                | 2.2                                | 1.34                          | 1                      |
| Miocene andesite      | 15%                | 2.6                                | 2.01                          | 1                      |
| Miocene sediments     | 11%                | 2.1                                | 2.60                          | 1                      |
| Miocene pyroclastics  | 10%                | 2.6                                | 2.76                          | 1                      |
| Pre-tertiary basement | 2%                 | 2.7                                | 2.60                          | 1                      |

Table 2. Permeabilities of the various geological formations in the simulation model.

| FORMATION             | ABSOLUTE FORMATION PERMEABILITY (MILLIDARCIES) |         |             |         |          |         |
|-----------------------|--|---------|-------------|---------|----------|---------|
|                       | East-West                                      |         | North-South |         | Vertical |         |
|                       | minimum  | maximum | minimum     | maximum | minimum  | maximum |
| Quaternary sediments  | 20   | 20      | 15          | 15      | 0.1      | 0.1     |
| Quaternary dacite     | 5  | 5       | 0.05        | 0.05    | 0.01     | 0.01    |
| Miyazawa pyroclastics | 0.05   | 5       | 0.0375      | 5       | 0.0005   | 0.25    |
| Akazawa pyroclastics  | 0.25   | 5       | 0.25        | 5       | 0.005    | 15      |
| Pleistocene sediments | 20   | 20      | 0.5         | 0.5     | 5        | 5       |
| Pleistocene andesite  | 0.1  | 5       | 0.1         | 5       | 0.005    | 1.5     |
| Pliocene pyroclastics | 2.5  | 20      | 1           | 20      | 0.005    | 20      |
| Miocene andesite      | 1.5  | 20      | 1           | 20      | 0.05     | 20      |
| Miocene sediments     | 0.01   | 10      | 0.05        | 0.5     | 0.005    | 0.005   |
| Miocene pyroclastics  | 0.0075   | 15      | 0.0075      | 25      | 0.005    | 10      |
| Pre-tertiary basement | 0.005  | 5       | 0.005       | 5       | 0.005    | 5       |

### Calculation of Reservoir Performance

The modeling study (Nakanishi and Iwai, 2000) involved numerous calculations, varying the various unknown parameters in the model, until a good match was obtained with both the natural-state (pre-1975) conditions in the reservoir (mainly pressures and temperatures) and the fluid production history from the field during the 1975-1996 interval (mainly

discharge enthalpies from the production wells). Fig. 5 shows the historical total production and injection rates (as well as the fixed post-1996 flow rates used for forecasting purposes). Individual well flow rate histories were imposed for each well in appropriate grid blocks as time-dependent mass sources and sinks. The history illustrated in Fig.5 involves two distinct phases. Between 1975 and 1982, total production and injection rates are relatively low but “net production” is still substantial. This is because, during this period, fluid was obtained using shallow wells which produced a high-enthalpy mixture of water and steam. Later, both the total fluid production and injection rates increase substantially after the new deviated production wells were drilled. Since the new wells feed from the deeper all-liquid portion of the reservoir, discharge enthalpies (and steam/water ratios) are lower than for the earlier shallow wells.

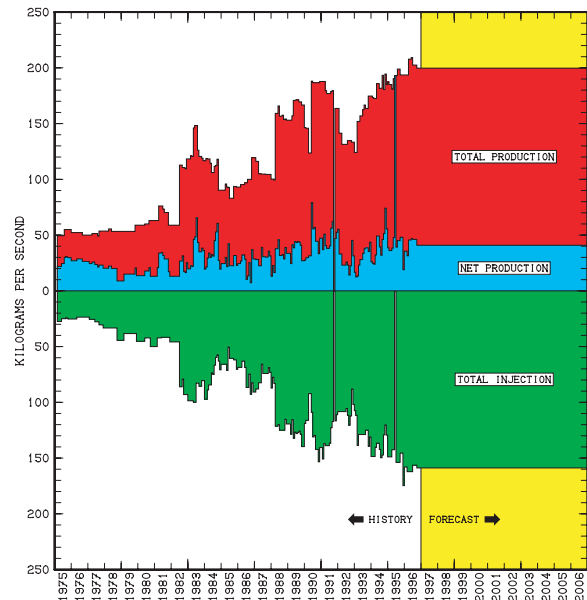


Figure 5. Time-histories of total fluid production (upper), injection (lower) and net production.

Most of the interior grid volume was modeled as an heterogeneous “porous medium”. Within a region surrounding the Onikobe wellfield (-12 km E <x<-9 km E, -131.5 km N <y<-134 km N; total 7.5 km<sup>2</sup>) the various rock formations were treated as double-porosity “fractured media” using the MINC representation (Pruess and Narasimhan, 1985; Pritchett, 1999), in the calculation of field exploitation. Fig.6 shows a representative example of results obtained from the final model. The observed changes in discharge enthalpies from deep well 131 exhibit the effects of cold reinjected water from nearby injection wells on the production well. The

values calculated by the model using the MINC treatment with a fracture spacing of 100 m show the same temporal trend as observed, although calculated values were slightly higher.

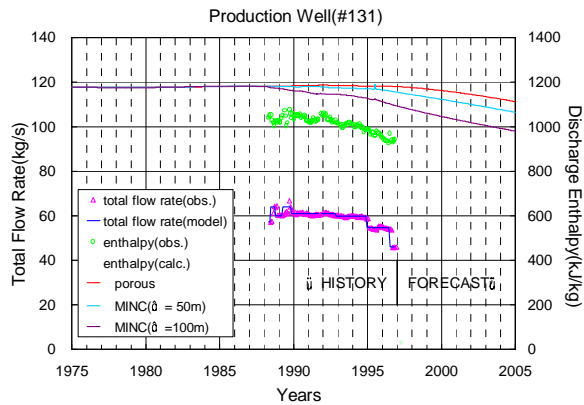


Figure 6. Enthalpy matching and imposed actual production flow rate, well 131.

Fig.7 illustrates the calculated time-history of total volume of steam in place in the computational grid volume. The initiation of field operations causes a significant increase in underground steam volume. Furthermore, most of this increase takes place during just the first few years of field operation.

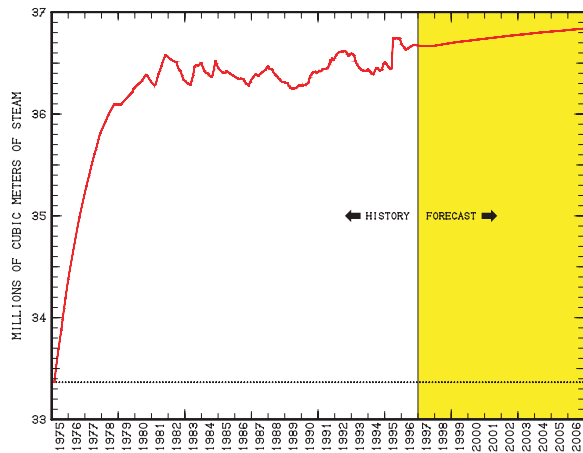


Figure 7. Time-history of total volume of steam in place in the computational grid volume.

### CHANGES IN SURFACE MICROGRAVITY

The STAR microgravity postprocessor (Pritchett, 1999) was next applied to the reservoir model to estimate the changes in surface microgravity arising from underground mass redistributions for the interval from 1 January 1975 to 1 January 2007. Unfortunately, no systematic records of microgravity changes have been maintained at Onikobe, so that there is no way to verify the calculated microgravity changes.

Fig.8 shows the calculated time-history of microgravity changes arising from reservoir-related phenomena (not including such effects as ground surface subsidence etc.) at a hypothetical observation station located in the southern part of the Onikobe project area (at -10.75 km E, -132.75 km N). At this location, gravity first decreases slightly for the first 30 months or so, and then begins to increase. The average rate of increase after 1985 is around four microgals per year at this location.

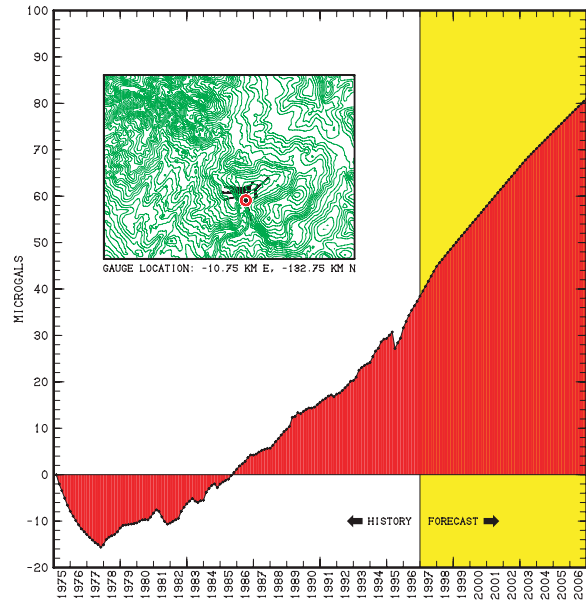


Figure 8. Computational changes in ground-surface microgravity as a function of time at a hypothetical station located within the borefield area.

Fig. 9 shows the spatial distribution of microgravity change (relative to natural-state conditions) on 1 January 1999, after 24 years of field operations. The principal feature is a region where gravity has increased (yellow-colored area), centered on the southern part of the project area. A relatively minor negative anomaly is also present slightly to the north. After the deeper production wells are brought on line, much greater amounts of liquid brine are injected into the reservoir than had been the case previously. As a result, significant increases in microgravity are observed in the reinjection area. Elsewhere, gravity disturbances are slight.

This microgravity distribution will not change very much in the future, according to these calculations. Microgravity is predicted to increase only at the rate of around four microgals per year (maximum) within the Onikobe project area. This suggests that most of the major changes in microgravity have already taken place, and the modest steam requirements of the

power station (only 12.5 MW) do not cause large changes in the underground fluid mass distribution in the field. Gravity disturbances of this magnitude will be difficult to distinguish from background effects such as changes in shallow groundwater level.

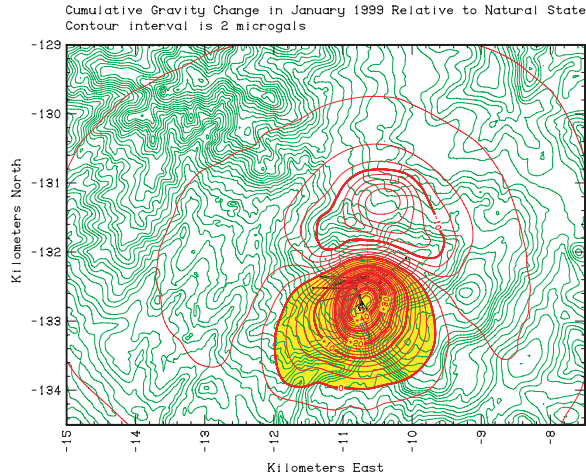


Figure 9. Computed changes in surface microgravity relative to the natural state on 1 January 1999, in microgals. Yellow color shows region of gravity increase.

## CHANGES IN SELF-POTENTIAL AT THE GROUND SURFACE

### Conditions for SP Calculations

A postprocessor has been developed for the STAR geothermal reservoir simulator to calculate distributions of electrical self-potential (“SP”) along the ground surface, and how they change in response to changes in underlying reservoir conditions (Ishido and Pritchett, 1999). In order to calculate the SP distribution a second “SP grid” is superimposed on the STAR grid used to calculate reservoir flow. The SP grid covers 324 km<sup>2</sup> (18 km × 18 km), centered on the middle of the study area. Vertically, the SP grid extends from the ground surface to -3.5 km ASL.

The boundary conditions on the SP grid are (1) zero potential at great distance (laterally and downward) and (2) zero normal potential gradient at the ground surface. Electrical resistivities throughout the entire SP grid volume were assigned to the various major geological formations at Onikobe based on the results of MT and CSAMT surveys. A model for computing the “drag current” (that is, a model for estimating the “zeta-potential” and how it will change; the fluid flow pattern is provided by the STAR simulation results) is also required. We used the model developed by Ishido and Mizutani (1981), and it was assumed that the flow paths have unit tortuosity. The

“ $\Delta pH$ ” parameter in the Ishido-Mizutani model was taken to be uniform and equal to -4.

### Changes in Ground Surface SP

Fig.10 shows the computed distribution of ground-surface self-potential (in millivolts) in the Onikobe study area in the natural-state (on 1 January 1975, prior to power station startup). A regional gradient of potential increasing from north to south is evident. Presumably, this broad feature is strongly influenced by the local topography, which should induce regional fluid flows (and the resulting electric currents) from the high ground to the north toward the lower-lying regions to the south.

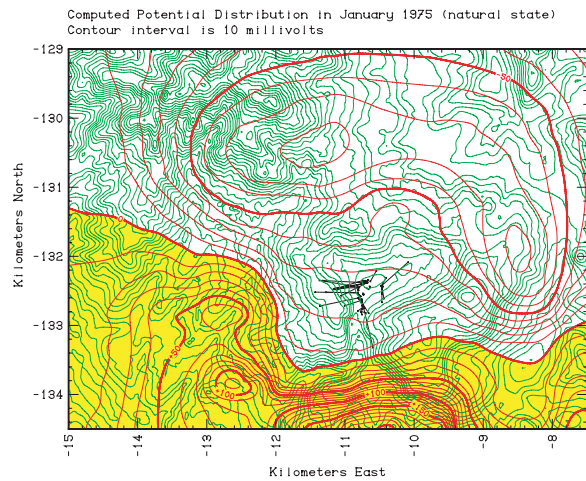


Figure 10. Computed ground-surface distribution of self-potential on 1 January 1975 (natural-state). Yellow zone indicates positive potential. Contour interval is 10 mV.

Fig.11 shows the cumulative changes in SP relative to the natural state on 1 January 1999 (the SP distribution on 1 January 1999 minus the initial

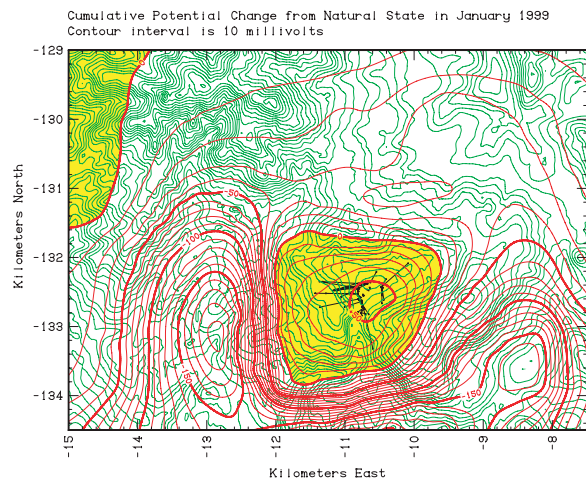


Figure 11. Cumulative computed change in ground-surface SP relative to the natural-state on 1 January 1999 (after 24 years). Regions where SP has increased are yellow. Contour interval is 10 mV.

distribution in Fig.10). Self-potential at the ground surface increases relative to the natural state in the immediate neighborhood of the wellfield, but decreases sharply in an annular circular zone surrounding the wellfield at a radius of 1 to 2 km, particularly in concentrated areas to the east and west. The pattern of changes in SP appears to reflect effects of production and injection in the wellfield itself and of downflowing recharge waters in the surrounding area.

Fig.12 shows a time-history of computed ground surface self-potential for a hypothetical station located within the wellfield (the same location as for the gravity history shown in Fig.8). The figure shows that the time-history of SP near the wells is extremely irregular. Comparing the SP history with the fluid production and injection rate histories in Fig.5 shows an extremely strong correlation between SP and fluid flow rates in the wells. Although the most pronounced SP changes take place at a distance from the wellfield (and are negative, approaching 200 mV in magnitude), substantial changes in surface SP started taking place in about 1983 in the wellfield itself, when the production strategy was changed from shallow to deep production.. This suggests that periodic or continuous SP measurements in the field could detect changes in subsurface flows, and could be useful for refinement of reservoir models.

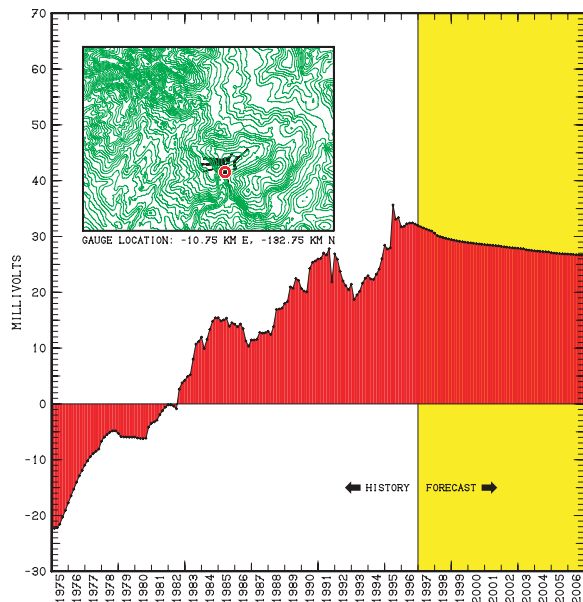


Figure 12. Computed changes in ground-surface SP as a function of time at a hypothetical station located within the borefield.

## SUMMARY

A feasibility study has been carried out to appraise the practicality of using geophysical techniques to detect and characterize subsurface changes induced in a geothermal reservoir by field operations, using a numerical reservoir model of the Onikobe field. Onikobe appears to be a marginal prospect for the future utilization of microgravity measurements for reservoir monitoring since most of the major changes in microgravity have already taken place in the mature field, and because of the modest steam requirements of the plant (12.5 MWe). It is estimated, on the other hand, that substantial changes in surface SP started taking place in about 1983, and that these changes are continuing to the present day and are strongly correlated with temporal fluctuations in the well flow rates.

## ACKNOWLEDGEMENTS

NEDO supported this work as part of the "New Sunshine Program" conducted by the Agency of Industrial Science and Technology (AIST) of the Japanese Ministry of International Trade and Industry (MITI). We also thank the management of EPDC for the permission to use proprietary data in this study.

## REFERENCES

- Abe, M. (1988), "Onikobe Geothermal Power Plant," In: *Geothermal Fields and Power Plants in Japan*, Symposium on Geothermal Energy, Kumamoto and Beppu, Japan, 49-56.
- Horikoshi, T., Nagahama, N. and Okubo, Y. (1998), "Reservoir Mass and Heat Flow Characterization," *Trans. Geotherm. Resour. Council.*, **22**, 165-169.
- Ishido, T. and Mizutani, H. (1981), "Experimental and Theoretical Basis of Electrokinetic Phenomena in Rock-water Systems and Its Applications to Geophysics," *Journal of Geophysical Research*, **86**, 1763-1775.
- Ishido, T., and Pritchett, J. W. (1999), "Numerical Simulation of Electrokinetic Potentials Associated with Subsurface Fluid," *Journal of Geophysical Research*, **104**, B7, 15,247-15,259.
- Klein, C. W., McNitt, J. R., Sanyal, S. K., Abe, M. and Nakanishi, S. (1990), "Corrosion vs. Temperature: Field development options at Onikobe

Geothermal Field, Miyagi Prefecture, Japan," *Trans. Geotherm. Resour. Counc.*, **14, Part II**, 1493-1499.

Nakanishi, S., Ariki, K., Pritchett, J. W. and Yamazawa, S. (2000), "Integrated Numerical Reservoir Modeling Coupled with Geophysical Monitoring Techniques," *Proc. World Geothermal Congress 2000*, Japan. (in press)

Nakanishi, S. and Iwai, N. (2000), "Reservoir Simulation Study of the Onikobe Geothermal Field, Japan," *Proc. World Geothermal Congress 2000*, Japan. (in press)

Pritchett, J. W. (1995), "STAR: A Geothermal Reservoir Simulation System," *Proc. World Geothermal Congress 1995*, Florence, 2959-2963.

Pritchett, J. W. (1999), "STAR User's Manual," *Revision F*, Maxwell Technologies Report No. SSS-TR-92-13366.

Pritchett, J. W., Wannamaker, P. E., Nakanishi, S. and Yamazawa, S. (2000), "Theoretical Feasibility Studies of Reservoir Monitoring Using Geophysical Survey Techniques," *Proc. World Geothermal Congress 2000*, Japan. (in press)

Pruess, K. and Narasimhan, T. N. (1985), "A Practical Method for Modeling Fluid and Heat Flow in Fractured Porous Media," *Soc. Pet. Eng. J.*, February, 14-26.